

Orbital Kondo effect in Cobalt-Benzene sandwich molecules

M. Karolak,¹ D. Jacob,² and A. I. Lichtenstein¹

¹*I. Institut für Theoretische Physik, Universität Hamburg, Jungiusstraße 9, D-20355 Hamburg, Germany*

²*Max-Planck-Institut für Mikrostrukturphysik, Weinberg 2, 06120 Halle, Germany*

(Dated: October 29, 2018)

We study a Co-benzene sandwich molecule bridging the tips of a Cu nanocontact as a realistic model of correlated molecular transport. To this end we employ a recently developed method for calculating the correlated electronic structure and transport properties of nanoscopic conductors. When the molecule is slightly compressed by the tips of the nanocontact the dynamic correlations originating from the strongly interacting Co $3d$ shell give rise to an orbital Kondo effect while the usual spin Kondo effect is suppressed due to Hund's rule coupling. This non-trivial Kondo effect produces a sharp and temperature-dependent Abrikosov-Suhl resonance in the spectral function at the Fermi level and a corresponding Fano line shape in the low bias conductance.

The discovery of ferrocene and bisbenzene chromium [1] over half a century ago was the starting point for experimental and theoretical work both in chemistry and physics concerning the intricate properties of organometallic compounds. The investigation of these and related sandwich complexes is driven by their relevance in various chemical applications (e.g. catalysis) and more recently also because of their magnetic properties (molecular magnets [2]) and their possible role in spintronic devices [3].

Apart from possible future nanotechnological applications, molecules containing a transition metal (TM) center coupled to aromatic groups are also of high interest from a fundamental point of view. The strong electronic correlations in the d shell of the transition metal can modify the ground state and electronic transport properties of such molecules, leading to many-body phenomena like the Kondo effect [4] as recently observed in TM-phthalocyanine molecules [5]. The importance of dynamical correlations in nanoscopic devices in general is further substantiated by the recent observation of Kondo-Fano line shapes in the low-voltage conductance of nanocontacts made from transition metals [6, 7].

While the Kondo effect is commonly associated with the screening of a local magnetic moment by the conduction electrons, it is also possible that another internal degree of freedom of an impurity or quantum dot coupled to conduction electrons gives rise to a Kondo effect [8]. One example is the so-called *orbital Kondo effect* where the pseudo-spin arising from an orbital degeneracy is screened instead of the real electron spin [9].

Such complex many-body phenomena call for a theoretical description beyond the standard treatment with Kohn-Sham density functional theory (KS-DFT) which cannot capture many-body physics beyond the effective mean-field picture. In order to account for the effects of electronic correlations on the electronic structure and transport properties of nanoscopic systems, it is therefore necessary to extend the conventional KS-DFT based transport methodology for nanoscopic conductors (see e.g. Ref. 10 and references therein). The incorrect be-

havior of the KS-DFT for strongly correlated systems can be remedied by augmenting the DFT with a local Hubbard-like interaction. This DFT++ approach is the de facto standard in the theory of solids [11, 12]. Recently this approach has been adapted to the case of nanoscopic conductors [7, 13–17].

In this letter we apply this methodology to investigate the transport properties of cobalt benzene sandwich molecules $(\text{C}_6\text{H}_6)\text{Co}(\text{C}_6\text{H}_6)$ (CoBz₂ in the following). We find that dynamical correlations in the Co $3d$ shell lead to the appearance of a sharp temperature-dependent resonance in the spectral function at the Fermi level commonly associated with the Kondo effect. We find that the Kondo resonance arises from an *orbital Kondo effect* in a doubly degenerate level of the Co $3d$ shell while the usual spin Kondo effect is suppressed due to the Hund's rule coupling.

We consider a single CoBz₂ molecule in contact with two semi-infinite copper nanowires as shown in Fig. 1a. The CoBz₂ molecule is the smallest instance of a general class of $\text{M}_n\text{Bz}_{n+1}$ complexes, where M stands for a metal atom, that have been prepared and investigated [3, 18]. The semi-infinite Cu wires exhibit the hexagonal symmetry of the molecule and correspond to the (6,0) wires described in Ref. 19. We investigate the system at three different Cu-tip-Co distances starting from the distance of metal ions in a CoBz-polymer, 3.6 Å, where the Cu tip atom takes the place of the would-be metal center of the next molecule in the polymer and also at the larger distances 4.0 Å and 4.3 Å (see Fig. 1a,b).

We perform DFT calculations using the CRYSTAL06 code [20] employing the LDA [21], PW91 [22] and the hybrid functional B3LYP [23], and using the all electron Gaussian 6-31G basis set. The geometries of the wires were relaxed beforehand and kept fixed during the calculations. The geometry of the Molecule in contact with the wires was relaxed employing the B3LYP functional. As can be seen from Fig. 1b the Bz-Bz distance h varies between 3.4 Å and 3.65 Å depending on the distance d of the Cu tip to the Co atom in the center of the molecule. At distances $d = 3.6$ Å and $d = 4.0$ Å the molecule is

slightly compressed compared to its *free* height of about $h = 3.6$ Å, whereas it is slightly stretched at $d = 4.3$ Å.

In order to capture many-body effects beyond the DFT level, we have applied the DFT+OCA (Density Functional Theory + One-Crossing Approximation) for nanoscopic conductors developed by one of us in earlier work [7, 15]. As a first step a calculation using a large periodic unit cell consisting of 8 lead layers is performed. This periodic unit cell is later extended by two semi-infinite Cu nanowires. This so-called supercell approach, is already described elsewhere in detail [7, 15, 16].

We are mostly interested in the properties of the Co 3*d* shell which exhibits strong electronic correlations. The hexagonal symmetry leads to a lifting of the degeneracy of the five 3*d* orbitals. The symmetry adapted representations are: the A_1 group consisting of the $d_{3z^2-r^2}$ orbital only, the doubly degenerate E_1 group consisting of the d_{xz} and d_{yz} orbitals and the E_2 group consisting of the d_{xy} and $d_{x^2-y^2}$ orbitals. Since the 6-31G basis set represents the *d* shell with 10 basis functions the 3*d* part of the on-site Hamiltonian on the Co atom is diagonalized to obtain the symmetry adapted five orbital crystal field basis for the problem.

Let us first discuss the DFT results. Figs. 1c+d show the imaginary parts of the hybridization functions obtained from the LDA electronic structure (see e.g. Ref. 7 for how to compute $\Delta_d(\omega)$ from the DFT electronic structure) which describes the (dynamic) broadening of the Co 3*d* orbitals due to coupling to the rest system (i.e. benzene+leads). The imaginary part of the hybridization function exhibits a distinct peak close to the Fermi level (E_F) in the E_2 channel, whose position, width and height depend significantly on the molecular geometry, specifically on the Bz-Co distance. The other channels E_1 and A_1 show only a negligible hybridization close to E_F . The dominant feature stems, similarly as shown for graphene [15, 24] from hybridization with the π_z orbital state of the benzene rings. The feature does not depend qualitatively on the DFT functional used, as we have found the same feature within GGA and also in B3LYP calculations.

The projected density of states (PDOS) in the Co 3*d* shell shows peaks in the vicinity of E_F stemming from the E_1 and E_2 levels, see Fig. 1, where the E_1 set shows some weight at E_F . The E_2 and A_1 states do not contribute to states at E_F . At larger Cu-Co distances the molecular character of the levels becomes more apparent as they narrow. This subsequently leads to an increase in the population of the E_1 set from 2.82 *e* to 3.54 *e*. Conversely the density of states increases at smaller distances, due to the broadening of the E_1 levels through increased hybridization. The LDA transmission properties also reflect the structure of the PDOS. A broad feature around zero bias is found at 3.6 Å which subsequently narrows down to a peak at about -200 meV for 4.3 Å.

Let us now turn to the LDA+OCA results. The hybridization functions $\Delta_d(\omega)$ obtained from the LDA

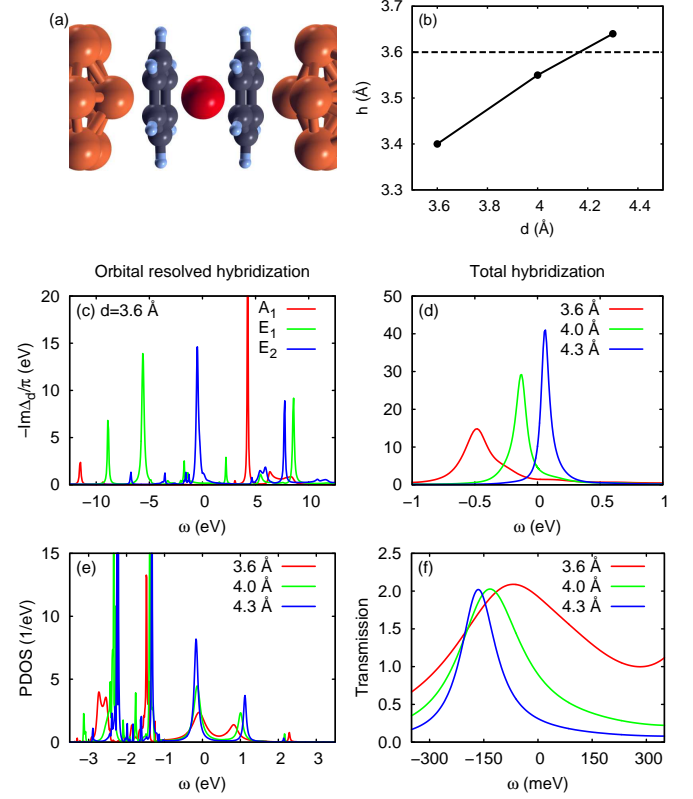


Figure 1. (Color online) (a) Atomic structure of CoBz₂ molecule in a Cu nanocontact. (b) Size h of CoBz₂ molecule as a function of the distance d between Co atom and Cu tip atoms. (c) Orbital resolved imaginary part of the hybridization function for $d = 3.6$ Å. (d) Total hybridization function (all Co 3*d* orbitals) for different d . (e) LDA Projected density of states for the Co 3*d* shell as a function of d . (f) LDA Transmission functions for different d .

mean-field description of the system, together with the interaction parameters $U = 5$ eV and $J = 1$ eV, and the energy levels ϵ_d define a generalized Anderson impurity model (AIM) with the Co 3*d* shell coupled to the rest of the system. The energy levels of the 3*d* orbitals are obtained from the KS Hamiltonian where as usual in DFT++ approaches a double counting correction (DCC) has to be subtracted to compensate for the overcounting of interaction terms. Here we employed the so-called fully localized or atomic limit double counting [25] $E_{dc} = U \cdot (N_{3d} - \frac{1}{2}) - J(\frac{N_{3d}}{2} - \frac{1}{2})$. The AIM is solved within the so-called One-Crossing Approximation (OCA) (see e.g. Refs. 11 and 26).

Fig. 2a compares the spectral functions of the Co 3*d* electrons calculated with the OCA impurity solver for the three distances considered here at high temperatures on a large energy scale. The spectra vary considerably as the distance d changes. Most importantly, for d around 3.6 Å when the molecule is slightly compressed, a sharp temperature-dependent peak appears right at E_F , as can

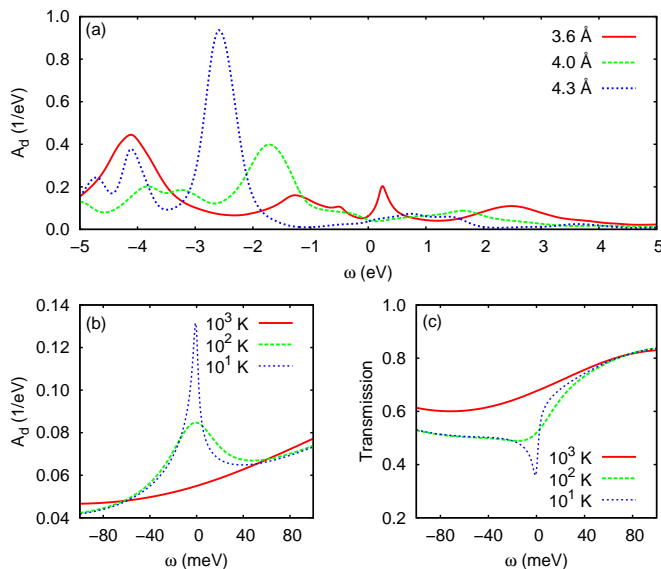


Figure 2. (Color online) (a) Spectral functions of Co 3d shell for different d at temperature $T \sim 1200$ K. (b,c) Spectral and transmission functions of the molecule at $d = 3.6$ Å for different temperatures.

be seen from Fig. 2b. The peak is strongly renormalized (i.e. it only carries a small fraction of the spectral weight) due to the strong electron-electron interactions. For larger distances $d \geq 4.0$ Å the sharp peak at E_F disappears indicating a drastic change in the electronic correlations.

The sharp peak in the spectral function at E_F that starts to develop already at temperatures of $kT = 0.01$ eV ≈ 120 K stems from the E_2 channel which is the only channel with appreciable hybridization near E_F , see Figs. 1b+c. Correspondingly, the transmission function (Fig. 2c) shows a Fano-like feature around zero energy. A renormalized, sharp and temperature-dependent resonance in the spectral function at E_F is commonly associated with the Kondo effect. Looking at the orbital occupations, we find that the E_2 channel that gives rise to the resonance for $d = 3.6$ Å has an occupation of about $2.8 e$ while the total occupation of the 3d shell is $N_d \sim 7.5 e$. The fractional occupation numbers indicate the presence of valence fluctuations where the charges in the individual impurity levels fluctuate in contrast to the pure Kondo regime where these fluctuations are frozen.

Analyzing the atomic states of the Co 3d shell contributing to the ground state of the system we find that the principal contribution ($\sim 45\%$) is an atomic state with 8 electrons and a total spin of $S = 1$ ($d^8, S = 1$) as shown in Fig. 3a. The total spin 1 stems from holes in the E_2 and A_1 channels. The charge fluctuations in the E_2 channel are mainly due to the contribution ($\sim 17\%$) of an atomic ($d^7, S = 3/2$) state. There are considerably weaker contributions ($\sim 4\%$) from atomic ($d^7, S = 1/2$) and ($d^9, S = 1/2$) states.

Note that the total spin $3/2$ of the principle d^7 atomic state is higher than the total spin 1 of the principal d^8 atomic state. Hence this fluctuation cannot flip the spin of the d^8 atomic state and therefore it cannot lead to a spin Kondo effect since the magnetic moment is not screened by these fluctuations. If a spin Kondo effect is to occur in this system it has to do so via a different mechanism. Two such mechanisms are conceivable here: one including the flipping of the total spin 1 of the principal d^8 atomic state and another mechanism involving only a flip of the spin $1/2$ within the E_2 shell. However, both roads to the spin Kondo are barred: First, the screening of the total spin 1 of the principal d^8 atomic state requires the (successive) flipping of two real spins (one in the A_1 and one in the E_2 level). The amplitude for such a processes is considerably smaller than the one involving a single spin-flip only [27]. Hence in general the Kondo scale decreases dramatically with increasing spin of the magnetic impurity. In addition, the A_1 level does not couple at all to the conduction electrons around E_F (no hybridization). Thus the spin $1/2$ associated with it cannot be flipped directly through hopping processes with the conduction electron bath. Hence a spin Kondo effect where the entire spin 1 of the Co 3d shell is screened is suppressed. Second, a Kondo effect where only the spin $1/2$ within the E_2 shell is screened, as illustrated in the lower panel of Fig. 3c, can be ruled out as well. Such a process requires fluctuations between the $S = 1/2$ configurations and the principle ($d^8, S = 1$) state. But due to the strong Hund's rule coupling of around 1 eV which couples the spin of the E_2 level to the spin of the A_1 level such a process is also strongly suppressed.

Nevertheless, the fluctuations between the ($d^8, S = 1$) and the ($d^7, S = 3/2$) states are primarily responsible for the three spectral features close to E_F including the sharp Kondo-like peak right at E_F , as illustrated in Fig. 3b. Also the broad peak around 4 eV below E_F originates from these fluctuations while the broad peak about 2.5 eV above E_F arises from fluctuations between the ($d^9, S = 1/2$) atomic state and the principal d^8 atomic state. The two peaks in the spectral function nearest to the Kondo resonance arise from the strong energy dependence of the hybridization function whose real part has poles just below and above E_F roughly at the positions of these two spectral features. Since a possible spin Kondo effect is suppressed we argue that the characteristic spectral features stem from an *orbital Kondo effect* in the doubly-degenerate E_2 levels of the Co 3d shell as illustrated in the upper panel of Fig. 3c. Here the index labeling the two orbitals with E_2 symmetry takes over the role of a pseudo spin. In the principal d^8 atomic state the E_2 levels are occupied with three electrons and hence have a pseudo spin of $1/2$. By excitation to the d^7 atomic state the electron with minority real spin and with some pseudo spin state is annihilated. By relaxation to the principal electronic d^8 state a minority real spin

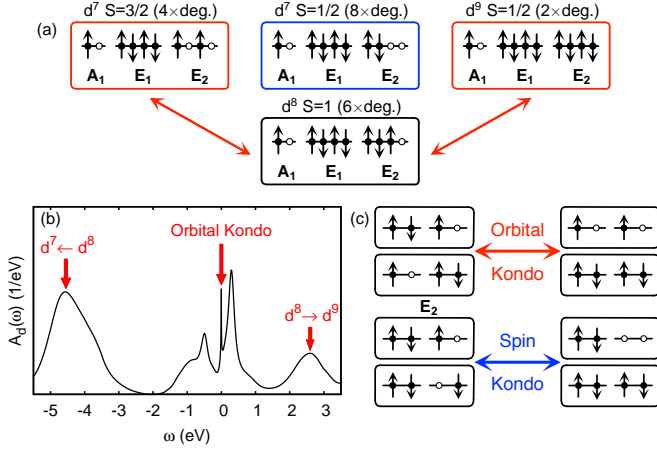


Figure 3. (a) Schematic picture illustrating the fluctuations between the atomic states that give rise to the spectral features shown in (b). (b) Spectral function around E_F for $d = 3.6$ Å. The arrows indicate the spectral features arising from the fluctuations between atomic states shown in (a). (c) Schematic illustration of the orbital (red) and spin flip processes (blue) responsible for the orbital and a (hypothetical) spin Kondo effect in the doubly-degenerate E_2 channel.

electron can now be created in one of the two pseudo spin states. Those processes that lead to a flip of the pseudo spin then give rise to the orbital Kondo effect and the formation of the Kondo peak at E_F .

We have also checked the dependence of the LDA+OCA spectra on the DCC. In general we find the spectra and also the Kondo peak to be qualitatively robust against shifts of the impurity levels in energy over a range of some electron volts. As expected for the Kondo effect the sharp resonance stays pinned to the Fermi level when shifting the impurity levels in energy, and only height and width somewhat change.

Stretching the molecule by displacing the tips of the Cu nanowires the Kondo resonance and the concomitant Fano line shape in the transmission disappear for distances $d \geq 4$ Å. This is accompanied by an increase of the occupation of the Co $3d$ shell. The new regime is characterized by a strong valence mixing between the d^8 and d^9 atomic state of roughly equal contribution indicating that the system is now in the so-called mixed valence regime (see e.g. Ref. 4, Chap. 5). Hence the orbital Kondo effect and the associated spectral features can be controlled by stretching or compressing the molecule via the tip atoms of the Cu nanocontact.

We have investigated the electronic and coherent transport properties of a CoBz₂ sandwich molecule in contact with copper nanowires. To this end we have employed a recently developed LDA+OCA method for nanoscopic conductors. The dynamic correlations originating from the coupling between the strongly interacting $3d$ electrons and the conduction electrons of the Cu nanowires

via p_z orbitals of the benzene rings give rise to an orbital Kondo effect in the Co E_2 levels. The orbital Kondo effect is accompanied by the appearance of a sharp, temperature dependent resonance in the spectral function at the Fermi level and a corresponding Fano line shape in the low-bias conductance. The appearance of this effect can be controlled by stretching or compressing the molecule with the Cu nanocontact tips.

We thank K. Haule for providing us with the OCA impurity solver and for helpful discussions. Support from SFB 668, LEXI Hamburg and ETSF are acknowledged. MK gratefully acknowledges the hospitality of the Max-Planck-Institute in Halle (Saale).

-
- [1] T. Kealy and P. Pauson, *Nature* **168**, 1039 (1951); E. Fischer and W. Hafner, *Z. Naturforsch., Part B* **10**, 665 (1955).
 - [2] D. Gatteschi, R. Sessoli, and J. Villain, *Molecular Nanomagnets* (Oxford University Press, 2006).
 - [3] H. Xiang *et al.*, *J. Am. Chem. Soc.* **128**, 2310 (2006); Y. Mokrousov *et al.*, *Nanotechnology* **18**, 495402 (2007).
 - [4] A. C. Hewson, *The Kondo problem to heavy fermions* (Cambridge University Press, 1997).
 - [5] A. Zhao *et al.*, *Science* **309**, 1542 (2005); L. Gao *et al.*, *Phys. Rev. Lett.* **99**, 106402 (2007).
 - [6] M. R. Calvo *et al.*, *Nature* **358**, 1150 (2009).
 - [7] D. Jacob, K. Haule, and G. Kotliar, *Phys. Rev. Lett.* **103**, 016803 (2009).
 - [8] D. L. Cox and A. Zawadowski, *Adv. Phys.* **47**, 599 (1998).
 - [9] O. Y. Kolesnychenko *et al.*, *Nature* **415**, 507 (2002); Jarillo-Herrero *et al.*, *ibid.* **434**, 484 (2005).
 - [10] D. Jacob and J. J. Palacios, *J. Chem. Phys.* **134**, 044118 (2011).
 - [11] G. Kotliar *et al.*, *Rev. Mod. Phys.* **78**, 865 (2006).
 - [12] A. I. Lichtenstein and M. I. Katsnelson, *Phys. Rev. B* **57**, 6884 (1998).
 - [13] P. Lucignano *et al.*, *Nature Mat.* **8**, 563 (2009).
 - [14] L. G. G. V. Dias da Silva *et al.*, *Phys. Rev. B* **80**, 155443 (2009).
 - [15] D. Jacob and G. Kotliar, *Phys. Rev. B* **82**, 085423 (2010).
 - [16] D. Jacob, K. Haule, and G. Kotliar, *Phys. Rev. B* **82**, 195115 (2010).
 - [17] R. Korytár and N. Lorente, arXiv:1102.1667v1.
 - [18] T. Kurikawa *et al.*, *Organometallics* **18**, 1430 (1999); A. Nakajima and K. Kaya, *J. Phys. Chem. A* **104**, 176 (2000); J. Martinez *et al.*, *J. Chem. Phys.* **132**, 044314 (2010).
 - [19] E. Tosatti *et al.*, *Science* **291**, 288 (2001).
 - [20] R. Dovesi *et al.*, CRYSTAL06, Release 1.0.2, Theoretical Chemistry Group - Università Di Torino - Torino (Italy).
 - [21] W. Kohn and L. J. Sham, *Phys. Rev.* **140**, A1133 (1965).
 - [22] J. P. Perdew and Y. Wang, *Phys. Rev. B* **33**, 8800 (1986).
 - [23] A. D. Becke, *J. Chem. Phys.* **98**, 5648 (1993).
 - [24] T. O. Wehling *et al.*, *Phys. Rev. B* **81**, 115427 (2010).
 - [25] M. T. Czyżyk and G. A. Sawatzky, *Phys. Rev. B* **49**, 14211 (1994).
 - [26] K. Haule *et al.*, *Phys. Rev. B* **64**, 155111 (2001).
 - [27] A. H. Nevidomskyy and P. Coleman, *Phys. Rev. Lett.* **103**, 147205 (2009).